**Title:** Local membrane charge regulates $\beta_2$ adrenergic receptor coupling to $G_i$

**Authors:** Strohman M.J.[1], Maeda S.[1], Hilger, D.[1], Masureel, M.[1], Du Y.[1], Kobilka B.K.[1*]

[1]Department of Molecular and Cellular Physiology, Stanford University School of Medicine, Stanford, California, USA

*Corresponding author

**Abstract**

G protein coupled receptors (GPCRs) are transmembrane receptors that signal through heterotrimeric G proteins. Lipid modifications anchor G proteins to the plasma membrane; however, little is known about the effect of phospholipid composition on GPCR-G protein coupling. The $\beta_2$ adrenergic receptor ($\beta_2$AR) signals through both $G_s$ and $G_i$ in cardiac myocytes where studies suggest that $G_i$ signaling may be cardioprotective. However, $G_i$ coupling is much less efficient than $G_s$ coupling in most cell-based and biochemical assays, making it difficult to study $\beta_2$AR-$G_i$ interactions. To investigate the role of phospholipid composition on $G_s$ and $G_i$ coupling, we reconstituted $\beta_2$AR in detergent/lipid mixed micelles and found that negatively charged phospholipids (PS and PG) inhibit $\beta_2$AR-$G_{i3}$ coupling. Replacing negatively charged lipids with neutral lipids (PC or PE) facilitated the formation of a functional $\beta_2$AR-$G_{i3}$ interaction that activated $G_{i3}$. $Ca^{2+}$, known to interact with negatively charged PS, facilitated $\beta_2$AR-$G_{i3}$ interaction in PS. Mutational analysis suggested that $Ca^{2+}$ interacts with the negatively charged EDGE motif on the carboxyl-terminal end of the αN helix of $G_{i3}$ and coordinates an EDGE-PS interaction. These results were confirmed in $\beta_2$AR reconstituted into nanodisc phospholipid bilayers. $\beta_2$AR-$G_{i3}$ interaction was favored in neutral lipids (PE and PC) over negatively charged lipids (PG and PS). In contrast, basal $\beta_2$AR-$G_s$ interaction was favored in negatively charged lipids over neutral lipids. In negatively-

charged lipids, $Ca^{2+}$ and $Mg^{2+}$ facilitated $\beta_2$AR-$G_{i3}$ interaction. Taken together, our observations suggest that local membrane charge modulates the interaction between $\beta_2$AR and competing G protein subtypes.

## Introduction

A third of all FDA approved pharmaceutical drugs function by modulating the activity of G protein coupled receptors (GPCRs)[1], a large receptor superfamily. GPCRs catalyze the activation of heterotrimeric G proteins, which in turn initiate a multitude of signaling cascades that alter cellular function.

G proteins are also a large superfamily, grouped into 4 subfamilies ($G_s$, $G_{i/o}$, $G_{q/11}$, $G_{12/13}$) encoded by 16 different genes[2]. Each subfamily activates distinct signaling pathways, and functional effects are cell-type specific. Most GPCRs can signal through more than one G protein subfamily, and ongoing research attempts to identify mechanisms that regulate G protein selectivity within a cell[2].

Here we investigate the dual G protein selectivity of the $\beta_2$ adrenergic receptor ($\beta_2$AR), a prototypical GPCR that mediates the fight-or-flight response. The dual G protein selectivity of $\beta_2$AR is best characterized in heart muscle (cardiac myocytes) where activation of $G_s$ increases contraction rate and activation of $G_i$ decreases it. $\beta_2$AR activity is stimulated by the hormone epinephrine. In healthy neonatal cardiac myocytes, epinephrine stimulated $\beta_2$AR immediately activates $G_s$, but after 10-15 minutes $\beta_2$AR signals predominantly through $G_i$[3]. Of interest, $G_i$ activation is impaired if $\beta_2$AR internalization is blocked[4]. Also, $G_i$ does not interact with a modified $\beta_2$AR that internalizes but does not recycle to the plasma membrane[5], and WT $\beta_2$AR that internalizes but is pharmacologically blocked from recycling[6]. Taken together, these

observations demonstrate that $\beta_2$AR-$G_i$ interaction is regulated spatially and temporally, and interaction occurs after epinephrine stimulated trafficking of $\beta_2$AR.

$\beta_2$AR-$G_i$ signaling plays a complex role in heart disease. While its anti-apoptotic effects[7,8] may prevent ischemic-reperfusion injury[9], $G_i$ activation comes at the price of decreased contractility, which is problematic in diseases where the heart is already sufficiently weakened, such as in heart failure[10], Takotsubo syndrome[11,12], and ischemia[13]. Notably, in heart failure $G_{i2}$ is upregulated[14-16], $\beta_1$AR (strictly $G_s$ coupled) is downregulated[17-20], while $G_s$[16], $G_{i3}$[16], and $\beta_2$AR[18] expression levels are unchanged. These changes may increase $\beta_2$AR-$G_{i2}$ coupling relative to the $\beta_2$AR-$G_s$ coupling.

The mechanism that initiates $\beta_2$AR-$G_i$ signaling in the healthy heart is not fully understood. Multiple biochemical mechanisms may play a role. PKA phosphorylation of $\beta_2$AR has been reported to increase $G_i$ coupling *in vitro*[21] and in HEK cells[22], but in cardiac myocytes, $\beta_2$AR-$G_i$ coupling is PKA independent[3]. In addition, GRK2 phosphorylation of $\beta_2$AR has been suggested to increase $G_i$ coupling[23], but other investigators have reported that dephosphorylation is critical for $\beta_2$AR recycling to the plasma membrane, and $\beta_2$AR-$G_i$ interactions[6]. Therefore, we sought to discover mechanisms that modulate $\beta_2$AR-$G_i$ coupling.

The epinephrine-stimulated trafficking of $\beta_2$AR (internalization and plasma membrane recycling) may influence the composition of phospholipids surrounding the $\beta_2$AR. It has been shown that negatively charged phospholipids stabilize an active conformation of the $\beta_2$AR and enhance its affinity for epinephrine[24]. Here we examine the effect of phospholipid charge on $\beta_2$AR interactions with $G_s$ and $G_i$.

## Results

Epinephrine activates $\beta_2$AR by stabilizing a conformation that is recognized by G protein. This conformation is partially stabilized by epinephrine and fully stabilized by the addition of G protein[25-27]. The conformational change can be detected using a modified $\beta_2$AR labeled on Cys265 at the cytoplasmic end of TM6 with an environmentally sensitive fluorophore, monobromobimane (mB-$\beta_2$AR, see methods)[28]. Epinephrine and G protein interaction red-shifts the emission maximum ($\lambda_{max}$, the wavelength where fluorophore emission intensity is greatest) and decreases the intensity of mB-$\beta_2$AR (Fig. 1a). Because $\lambda_{max}$ is independent of mB-$\beta_2$AR concentration, it is a more reliable indicator of $\beta_2$AR conformation than fluorescence intensity. We therefore monitored changes in $\lambda_{max}$ of mB-$\beta_2$AR to detect G protein coupling.

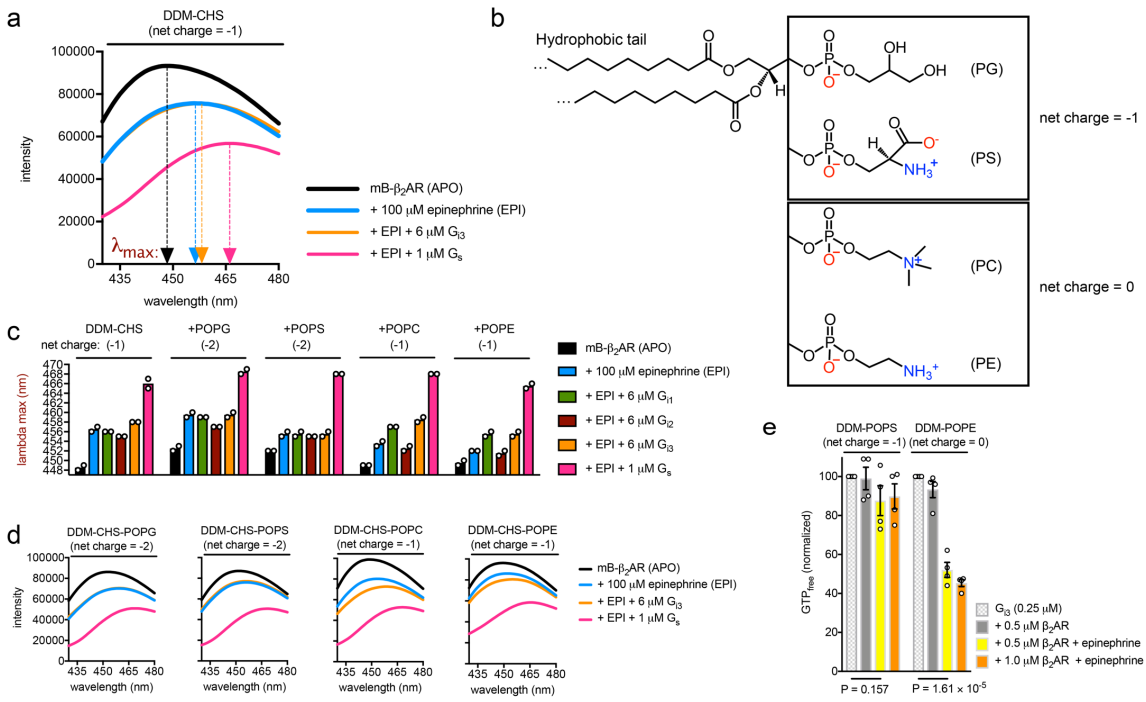


Figure 1. **Effect of phospholipids on mB-$\beta_2$AR-G protein interaction in DDM mixed micelles**

**a.** mB-$\beta_2$AR emission spectra in the presence and absence of epinephrine and G protein ($G_s$ and $G_{i3}$) in DDM-CHS micelles (4:1 DDM:CHS). Arrows point to the lambda max value, i.e. the wavelength where mB emission intensity is greatest.

**b.** Structure of phospholipids, categorized by their net charge: Phosphatidylglycerol (PG) and phosphatidylserine (PS) have a net charge of -1. Phosphatidylcholine (PC) and phosphatidylethanolamine (PE) have a net charge of 0 (i.e. net neutral). Negatively charged groups highlighted in red. Positively charged groups highlighted in blue.

**c.** mB-$\beta_2$AR interaction with epinephrine and G protein ($G_{i1}$, $G_{i2}$, $G_{i3}$, and $G_s$) as assessed by changes in mB lambda max. Interaction was assessed in DDM-CHS micelles (4:1 DDM:CHS) and in DDM-CHS micelles containing POPG, POPS, POPC, or POPE lipids (3:1:1 DDM:CHS:Lipid).

**d.** Selected mB-$\beta_2$AR emission spectra from panel C, showing spectra shifts induced by epinephrine, $G_{i3}$, and $G_s$.

**a-d.** The indicated net charges are net molecular charge, not net micelle charge. CHS, POPG, and POPS each have a net charge of -1. DDM, POPC, and POPE are net neutral. mB-$\beta_2$AR concentration is 300 nM. Data are mean of two independent experiments.

**e.** GTP turnover in the presence and absence of $\beta_2$AR (0.5 μM vs. 1 μM) and saturating epinephrine, in 4:1 DDM:POPS vs. 4:1 DDM:POPE. Data were normalized relative to turnover by $G_{i3}$ (0.25 μM) in the absence of $\beta_2$AR (shown in Supplementary figure 3). Data are mean +/- s.e.m of four independent experiments. Statistical significance was determined by using a two-sided Student's *t*-test.

**Negatively charged phospholipids decrease $\beta_2$AR coupling to $G_i$**

In the presence of epinephrine, we observe a change in intensity and $\lambda_{max}$ of mB-$\beta_2$AR following the addition of $G_s$ in a detergent mixture containing n-dodecyl-β-D-maltopyranoside (DDM) and cholesteryl hemisuccinate (CHS) that is commonly used for biochemical study of GPCR/G protein complexes (Fig. 1a). In contrast, the coupling efficiency of mB-$\beta_2$AR-$G_{i3}$ was relatively weak (Fig. 1a). Next, we compared the coupling efficiency of mB-$\beta_2$AR-$G_i$ in DDM-CHS mixtures with different phospholipids incorporated (Fig. 1b,c). While we were unable to detect interactions of mB-$\beta_2$AR with $G_{i1}$, $G_{i2}$ or $G_{i3}$ in the presence of negatively charged lipids (POPS and POPG), we observed a weak interaction with $G_{i1}$ and $G_{i3}$ in neutral lipids (POPE and POPC) (Fig. 1c,d). This result suggested that negatively charged lipids may repel $G_{i1}$ and $G_{i3}$ interaction with $\beta_2$AR, despite the fact that negatively charged lipids enhance epinephrine binding affinity, as previously reported[24]. Given that mB-$\beta_2$AR-$G_{i1}$ and mB-$\beta_2$AR-$G_{i3}$ interaction appeared comparable, we narrowed our focus on mB-$\beta_2$AR-$G_{i3}$ interaction because $G_{i3}$ (not $G_{i1}$) is expressed in the heart[16].

We also observed that negatively charged CHS decreased mB-$\beta_2$AR-$G_{i3}$ coupling (Supplementary Fig. 1). This effect was minimized in acidic buffers known to protonate (and neutralize) CHS[29], supporting our hypothesis that negatively charged lipids decrease $\beta_2$AR-$G_i$ coupling. Given reports that PKA phosphorylation of $\beta_2$AR increases $\beta_2$AR-$G_i$ interaction *in vitro*[21], we also tested the effect of PKA phosphorylation, but no mB-$\beta_2$AR-$G_{i3}$ enhancement was observed (Supplementary Fig. 2), suggesting that phosphorylation does not potentiate $\beta_2$AR-$G_{i3}$ interaction under our experimental conditions, and that other mechanisms may enhance $\beta_2$AR-$G_{i3}$ interaction.

In subsequent experiments, we omitted negatively charged CHS in order to assess the effect of phospholipid charge on mB-$\beta_2$AR-$G_{i3}$ interactions. We tested whether the increased mB-$\beta_2$AR-$G_{i3}$ interaction we observed in neutral lipid represented functional interaction. Indeed, $\beta_2$AR stimulated GTP turnover was detected in DDM micelles containing POPE (net neutral lipid) but not in DDM micelles containing POPS (net negative) (Fig. 1e). This effect on $\beta_2$AR mediated turnover was significant, even though the lipid:DDM molar ratio was only 1:4. The lipid environment (POPS vs. POPE) did not affect basal GTP turnover by $G_{i3}$ (Supplementary Fig. 3). Taken together, these results indicate that the charge property of phospholipids regulates $G_i$ activation by $\beta_2$AR.

**$Ca^{2+}$ promotes $\beta_2$AR-$G_{i3}$ coupling in negatively charged phospholipids**

$Ca^{2+}$, a ubiquitous second messenger, plays an important role in cardiac myocytes; $Ca^{2+}$ waves, magnified by $G_s$ activation, drive the cardiac myocyte contraction machinery. Recently $Ca^{2+}$ was reported to regulate T cell receptor activation by modulating the charge property of lipids[30]. Given that $Ca^{2+}$ interaction with negatively charged phospholipids screens the negative charge, we tested whether $Ca^{2+}$ improves mB-$\beta_2$AR-$G_{i3}$ coupling efficiency in negatively charged DDM-POPS. Indeed, $Ca^{2+}$ improved coupling efficiency in DDM-POPS micelles (Fig. 2a), and this effect required POPS (Fig. 2b). Moreover, $Ca^{2+}$ had little effect on mB-$\beta_2$AR-$G_s$ interaction, implicating differences in $G_s$ and $G_{i3}$ surface charge.

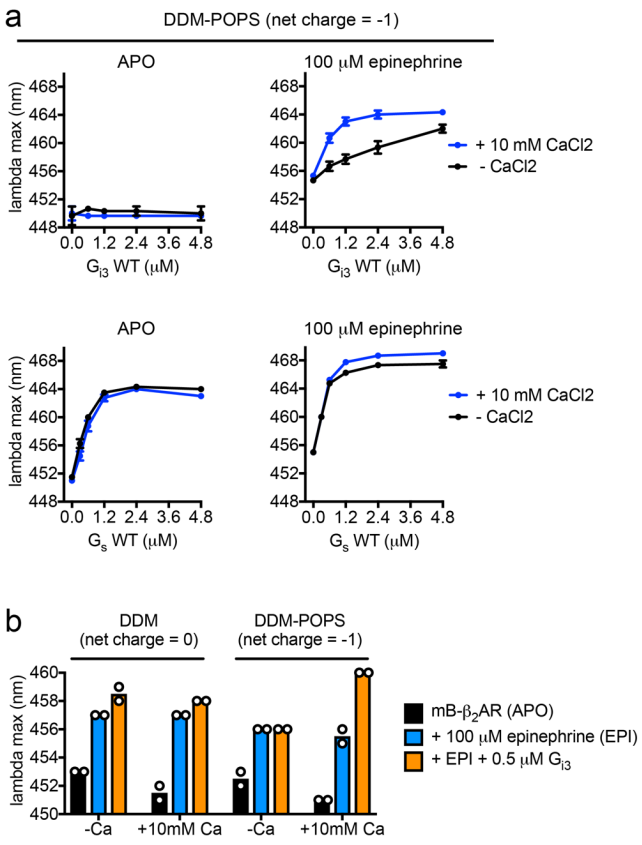


Figure 2. **The effect of $Ca^{2+}$ on $\beta_2$AR-$G_{i3}$ and $\beta_2$AR-$G_s$ interaction in micelles containing negatively charged phosphatidylserine (POPS)**

**a.** The effect of 10 mM CaCl2 on mB-$\beta_2$AR-G protein interaction ($G_{i3}$ and $G_s$) was examined in micelles containing 4:1 DDM:POPS. Data were collected in the absence (left) and presence (right) of epinephrine. mB-$\beta_2$AR concentration is 250 nM. Data are mean +/- s.e.m of three independent experiments.

**b.** The effect of 10 mM CaCl2 on mB-$\beta_2$AR-$G_{i3}$ interaction in DDM micelles +/- POPS (i.e. 100% DDM vs. 3:2 DDM:POPS). mB-$\beta_2$AR concentration is 250 nM. Data are mean of two independent experiments.

## $Ca^{2+}$ interacts with the amino terminal helix of $G_{i3}$

Next, we sought to determine the mechanism by which $Ca^{2+}$-POPS interactions increase mB-$\beta_2$AR coupling to $G_{i3}$ but not to $G_s$. Given that the amino terminal helix (αN) of G protein is adjacent to the membrane when coupled to the $\beta_2$AR[27], and polybasic residues

on $G_s$ αN are known to facilitate membrane interaction[31], we looked for a possible selectivity determinant within αN. Given αN of $G_s$ and $G_i$ are differentially charged (Fig. 3a), we first replaced αN of $G_s$ with αN of $G_{i3}$, creating a $G_{i3}$-$G_s$ chimera (Fig. 3b).

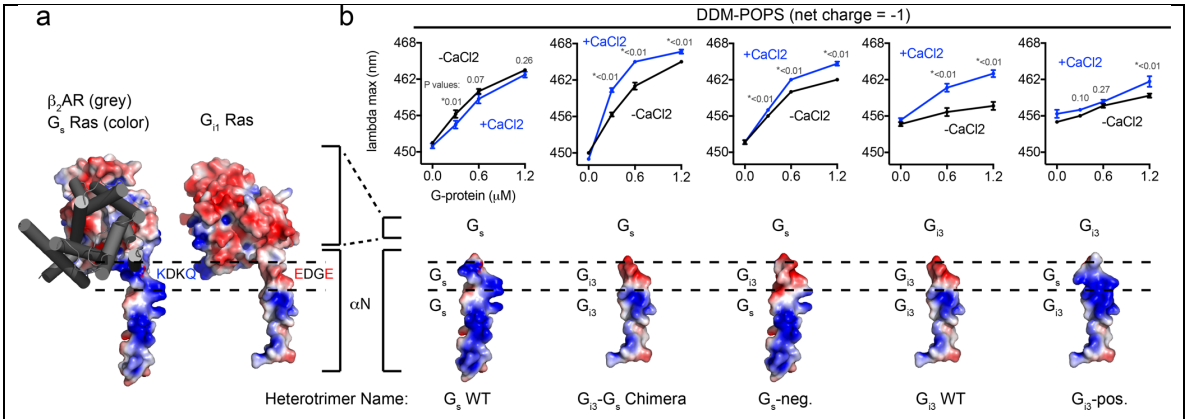


Figure 3. **The effect of $Ca^{2+}$ on mB-$\beta_2$AR interaction with G protein charge mutants**

**a.** Models of the membrane-facing surfaces of the Ras domains of $G_s$ (PDB: 3SN6) and $G_{i1}$ (1GP2). The membrane-facing surface of $G_{i1}$ was modeled by superimposing the Ras domain of Gi1 onto the structure of $G_s$ in complex with $\beta_2$AR (PDB: 3SN6). Red and blue signify negative and positive charge, respectively. $\beta_2$AR is shown in grey. Dashed lines highlight the region in αN where charge differs: The sequence is KDKQ in WT $G_s$ vs. EDGE in WT $G_{i1}$ (and in $G_{i2}$, $G_{i3}$).

**b.** mB-$\beta_2$AR-G protein dose-response curves +/- 10 mM CaCl2. Data were generated with the G protein mutant depicted below the curves: mutations were made in αN and corresponding electrostatic models are shown. Epinephrine was not included in experiments titrating $G_s$ WT, $G_{i3}$-$G_s$ Chimera, or with $G_s$-neg. to enhance the effect of CaCl2. Epinephrine (100 μM) was included in experiments titrating $G_{i3}$ WT and $G_{i3}$-pos. mB-$\beta_2$AR concentration is 250 nM. Data are mean +/- s.e.m of three independent experiments. Statistical significance was determined by using a two-sided Student's *t*-test. Test assesses the effect of CaCl2 at each G protein concentration.

While $Ca^{2+}$ does not promote mB-$\beta_2$AR coupling to WT Gs (Fig. 3b), it did promote mB-$\beta_2$AR coupling to the $G_{i3}$-$G_s$ chimera (Fig. 3b). Next, we compared the membrane-facing charge of $G_s$ WT αN and $G_{i3}$ WT αN. Structural analysis revealed that charge differed at the C terminal end of αN: $G_i$ harbors a negatively charged motif (EDGE) at the position where $G_s$ harbors a positively charged motif (KDKQ) (Fig 3a). To examine whether this motif dictates a differential response to $Ca^{2+}$, we constructed a $G_s$ mutant ("$G_s$-neg.") containing the negatively charged motif of $G_{i3}$ (KDKQ→EDGE). $Ca^{2+}$ increased mB-$\beta_2$AR interaction with this mutant (Fig 3b), suggesting the EDGE motif is responsible for the

effect of $Ca^{2+}$ on $G_{i3}$ αN. Taken together, our results imply that $Ca^{2+}$ coordinates an interaction between the negatively charged EDGE motif on αN of $G_{i3}$ and the headgroup of POPS. In the absence of $Ca^{2+}$, like-charge repulsion decreases mB-$\beta_2$AR coupling to $G_{i3}$.

We also constructed a $G_{i3}$ mutant ("$G_{i3}$-pos.") containing the positively charged motif of $G_s$ (EDGE→KDKQ). The mutations only partially removed the effect of $Ca^{2+}$ (Fig. 3b), indicating the effect of $Ca^{2+}$ on $G_{i3}$ extends beyond an effect on αN (see discussion).

**Bilayer charge is a tunable modulator of the G protein subtype selectivity**

To examine the effects of phospholipids in a more native environment, we reconstituted mB-$\beta_2$AR into nanodisc bilayers and purified the nanodiscs to homogeneity using size-exclusion chromatography (Supplementary Fig. 4).

First, we compared the influence of lipid composition in the absence of $Ca^{2+}$. Negatively charged bilayers (DOPG and DOPS bilayers) red-shifted the emission spectra of mB-$\beta_2$AR alone, suggesting negatively charged bilayers stabilize mB-$\beta_2$AR in an active conformation, as has been previously reported[24]. While negatively charged bilayers increased mB-$\beta_2$AR coupling to $G_s$ (Fig. 4), negatively charged bilayers (especially DOPS bilayers) decreased mB-$\beta_2$AR coupling to $G_{i3}$ (Fig. 4).

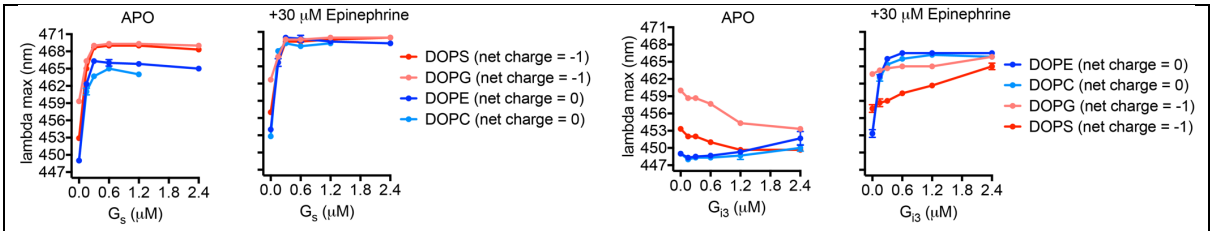


Figure 4. **Effect of phospholipid bilayer charge on mB-$\beta_2$AR-$G_{i3}$ and mB-$\beta_2$AR-$G_s$ interaction.** The effect of $G_s$ (left) and $G_{i3}$ (right) concentration on mB-$\beta_2$AR fluorescence was examined in nanodisc bilayers of varying phospholipid composition (DOPE, DOPC, DOPG, or DOPS). Net charge of phospholipid indicated in parentheses. mB-$\beta_2$AR concentration is 100 nM; maximum stoichiometry is 24:1 (G protein:mB-$\beta_2$AR). Data are mean +/- s.e.m of three independent experiments.

In fact, in negatively charged bilayers without epinephrine, $G_{i3}$ unexpectedly *blue-shifted* the emission spectra of mB-$\beta_2$AR. While this may indicate that $G_{i3}$ stabilizes the $\beta_2$AR in an inactive conformation in negatively charged lipids, it may represent a non-specific interaction of inactive $G_{i3}$ with the $\beta_2$AR or the lipid bilayer.

Next we examined the effect of $Ca^{2+}$ and $Mg^{2+}$. In the absence of $G_{i3}$, both $Ca^{2+}$ and $Mg^{2+}$ reversed the active-state stabilizing effect of negatively charged DOPS and DOPG bilayers (Fig. 5a). In contrast, $Ca^{2+}$ and $Mg^{2+}$ increased mB-$\beta_2$AR coupling to $G_{i3}$ in negatively charged DOPS bilayers, but only $Ca^{2+}$ was efficacious at concentrations below 1 mM (Fig. 5a). $Ca^{2+}$ similarly affected mB-$\beta_2$AR-$G_{i3}$ interaction in negatively charged DOPG bilayers (Fig. 5a), but the magnitude of the effect in DOPG bilayers was less than observed in DOPS bilayers due to the higher baseline effect of DOPG on $\beta_2$AR conformation.

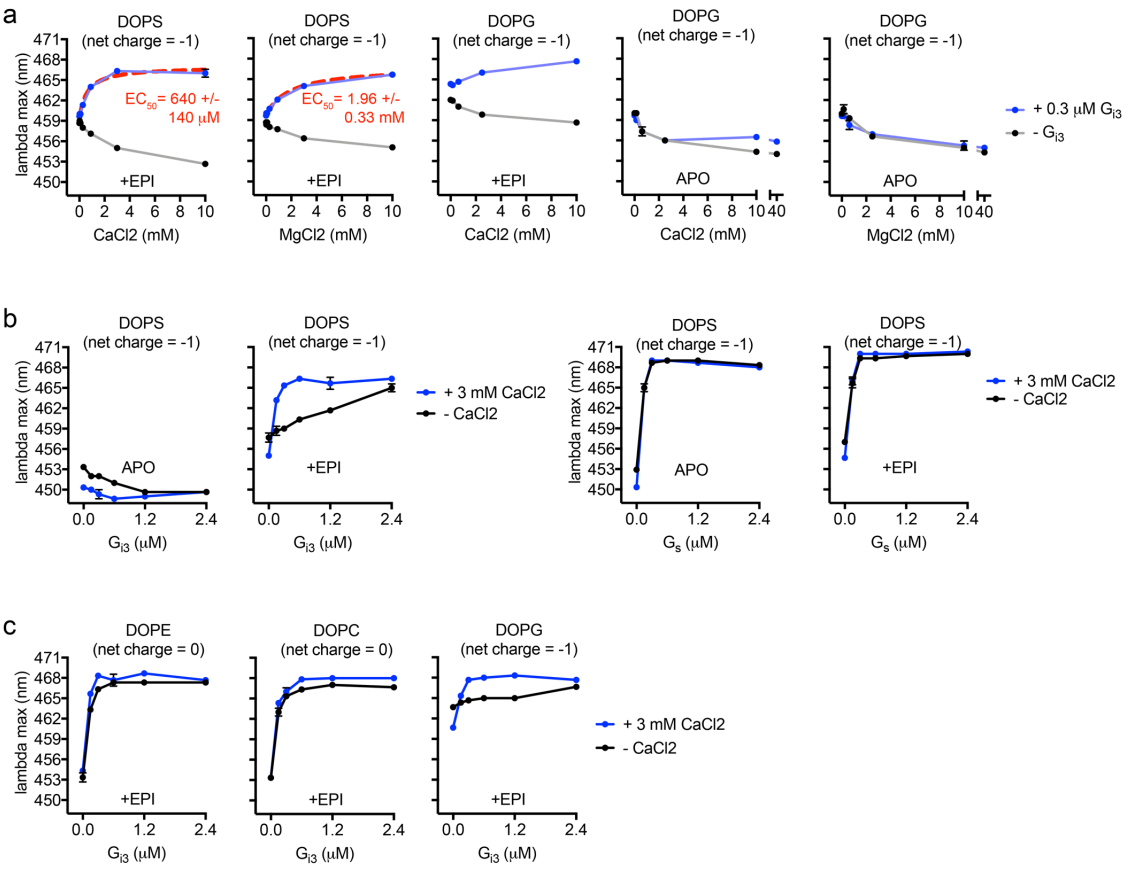


Figure 5. **Effect of $Ca^{2+}$ and $Mg^{2+}$ on mB-$\beta_2$AR-$G_{i3}$ and mB-$\beta_2$AR-$G_s$ interaction in nanodisc bilayers of varying charge**

**a.** The effect of CaCl2 and MgCl2 concentration on mB-$\beta_2$AR fluorescence in DOPS and DOPG nanodisc bilayers was examined in the presence and absence of $G_{i3}$. Epinephrine was included (30 μM) or omitted (APO). $EC_{50}$ is mean +/- s.e.m.

**b.** The effect of G protein concentration ($G_{i3}$ and $G_s$) on mB-$\beta_2$AR fluorescence +/- 3 mM CaCl2 was examined in DOPS nanodiscs in the presence of epinephrine (30 μM) or in its absence (APO).

**c.** The effect of $G_{i3}$ on mB-$\beta_2$AR fluorescence +/- 3 mM CaCl2 was examined in DOPE, DOPC, and DOPG nanodisc bilayers in the presence of 30 μM epinephrine (EPI).

**a-c.** mB-$\beta_2$AR concentration is 100 nM. Net charge of phospholipid molecule indicated in parentheses. Data are mean +/- s.e.m of three independent experiments.

We compared the effect of $Ca^{2+}$ on mB-$\beta_2$AR interactions with $G_s$ and $G_{i3}$ in DOPS bilayers. As observed in micelles, $Ca^{2+}$ increased mB-$\beta_2$AR coupling to $G_{i3}$ but not to Gs (Fig. 5b). $Ca^{2+}$ also improved mB-$\beta_2$AR-$G_{i3}$ coupling efficiency in negatively charged DOPG bilayers (Fig. 5c). Only a minor effect of $Ca^{2+}$ was observed in neutral DOPE and

DOPC bilayers (Fig. 5c & Supplementary Fig. 5), which could be attributable to weaker $Ca^{2+}$/DOPE and $Ca^{2+}$/DOPC interactions that have been reported[32]. Taken together, our results strongly suggest that $Ca^{2+}$ facilitates mB-$\beta_2$AR-$G_{i3}$ interaction but not mB-$\beta_2$AR-$G_s$ interaction. Moreover, these observations provide biochemical proof-of-concept that divalent cation/membrane interactions can increase $G_i$ coupling to the $\beta_2$AR.

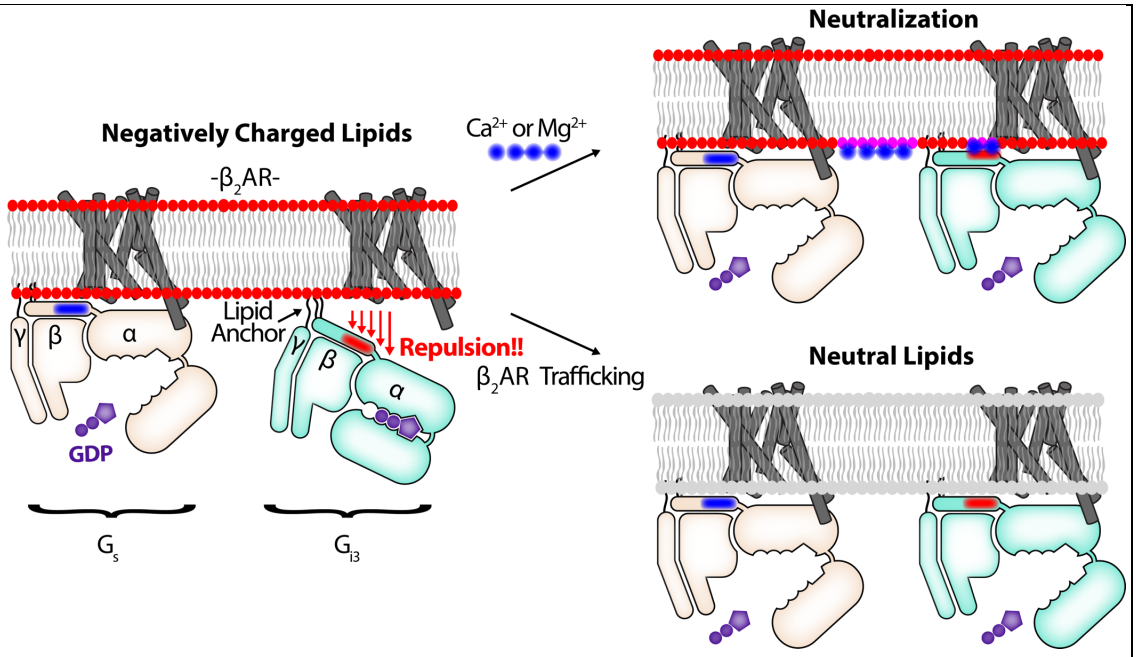


Figure 6. **Membrane charge is a tunable modulator of $\beta_2$AR-G protein interaction**
Models depict epinephrine-bound $\beta_2$AR.

**Left:** In negatively charged lipids, $\beta_2$AR-$G_s$ coupling is efficient, but $\beta_2$AR-$G_{i3}$ coupling is relatively inefficient, in part because $\beta_2$AR-$G_{i3}$ attraction is countered by membrane-$G_{i3}$ repulsion. Specifically, negatively charged lipids repel the negatively charged EDGE motif found on the amino terminal helix of $G_{i3}$ (shown in red), a region that is positively charged in $G_s$ (shown in blue).

**Right:** Two mechanisms that neutralize membrane charge facilitate $\beta_2$AR coupling to $G_{i3}$. These mechanisms may play a role in $G_s$-to-$G_i$ switching in cardiac myocytes. Top right: $Ca^{2+}$ and $Mg^{2+}$ stabilize a like-charge interaction between the membrane and the EDGE motif. (Note that the effect of $Ca^{2+}$ and $Mg^{2+}$ may extend beyond an effect on $\alpha$N positioning). Bottom right: Epinephrine stimulated $\beta_2$AR traffics to membrane without negatively charged lipids.

## Discussion

We observed that local membrane charge regulates $\beta_2$AR-G protein interaction. Negatively charged membrane promotes $\beta_2$AR-$G_s$ coupling and suppresses $\beta_2$AR-$G_{i3}$ coupling. However, $G_s$ bias is reduced in neutral membrane and in negatively charged membrane in the presence of divalent cations (see model in Fig. 6).

We have begun to explore the mechanism by which $Ca^{2+}$ increases mB-$\beta_2$AR coupling to $G_{i3}$ in PS phospholipids. Although G proteins are membrane tethered via lipidation, the lipid anchor of $G_{i3}$ is not sufficient for optimal interaction with $\beta_2$AR in negatively charged bilayers, possibly due to repulsion of the carboxyl terminal end of the αN helix. We propose that $Ca^{2+}$ helps orient the carboxyl terminal end of the αN helix of $G_{i3}$ near the membrane, thereby facilitating $\beta_2$AR-$G_{i3}$ interactions. More specifically, we propose that $Ca^{2+}$ facilitates the interaction of PS with the negatively charged EDGE motif on the αN helix of $G_{i3}$. $Ca^{2+}$ may stabilize the PS-EDGE interaction by coordinating a like-charge interaction between the carboxylate groups on $G_{i3}$ and the carboxylate group on PS (not present on PG) (refer to structures in Fig 1b). Alternatively, $Ca^{2+}$ might coordinate a like-charge interaction between the carboxylate groups on $G_{i3}$ and the phosphate group present on PS and PG, or $Ca^{2+}$ might coordinate an intramolecular interaction between the phosphate group and the carboxylate group on PS, “freeing” the amino group (NH3+) on PS to interact with the carboxylate groups on $G_{i3}$. Notably, the amino terminal helix (αN) of $G_{i1}$, $G_{i2}$, and $G_{i3}$ are similarly charged, and all three sequences contain the EDGE motif.

We have previously shown that negatively charged lipids, particularly PG, stabilize the $\beta_2$AR in an active-like conformation as revealed by changes in mB-$\beta_2$AR fluorescence and an increased affinity for agonists[24]. These effects are likely due to interactions between the lipids and positively charged amino acids on the $\beta_2$AR. Here we observed that the effect of DOPG and DOPS on mB-$\beta_2$AR can be reversed by both $Ca^{2+}$ and $Mg^{2+}$ (Fig. 5a). Yet, these divalent cations do not appear to reduce coupling to $G_s$.

$\beta_2$AR signals from caveolin-rich rafts[33,34] within T-tubules[35]. While $\beta_2$AR preferentially interacts with PG in insect cell membrane[24], the phospholipid composition immediately adjacent to $\beta_2$AR in T-tubules, and how it changes during $\beta_2$AR trafficking, is currently unknown. Net-neutral PC and PE are the major phospholipids in T-Tubules[36-38]. However, negatively charged PS is enriched in T-tubules relative to other membrane fractions (7.5-12.3% of total phospholipid)[36-40]. While cytosolic $Ca^{2+}$ concentrations are typically less than 1 mM[41], concentrations of $Ca^{2+}$ in the mM range may be observed in cardiac myocytes (discussed below).

Investigators have long speculated about the functional role of $Ca^{2+}$ in the cleft between T-tubule membrane (where $\beta_2$AR is localized) and juxtaposed sarcoplasmic reticulum (SR)[42-44]. During each action potential, extracellular $Ca^{2+}$ flows into the cleft through L-type $Ca^{2+}$ channels (LTCCs) on the plasma membrane and through ryanodine receptors (RyRs) on the sarcoplasmic reticulum[41]. Cleft $Ca^{2+}$ concentrations spark to > 100 μM in the absence of epinephrine and >1 mM[45,46] following epinephrine stimulation, a consequence of $G_s$ activation. Computational models show that negatively charged phospholipids buffer approximately half the $Ca^{2+}$ released into the cleft[45], and experiments have shown that 80% of inner-leaflet bound $Ca^{2+}$ is bound to negatively-

charged phospholipids[47]. Additionally, biochemical investigations show that $Ca^{2+}$ can cluster negatively charged PS[48] and PIP2[49,50] lipids.

$\beta_1$AR and $\beta_2$AR signaling through $G_s$ alters calcium handling in the cardiac myocyte, and increases the magnitude of $Ca^{2+}$ currents and $Ca^{2+}$ transients, which stimulate cardiac contraction[41,51]. However, elevated $Ca^{2+}$ concentrations also activate the $Ca^{2+}$/calmodulin-dependent protein kinase II (CaMKII), which is implicated in structural remodeling that ultimately results in cardiac dysfunction[52-56]. Several lines of evidence suggest $\beta_2$AR-$G_i$ signaling keeps $\beta_2$AR-$G_s$ signaling in check via negative feedback: $\beta_2$AR-$G_i$ signaling occurs minutes after $\beta_2$AR-$G_s$ signaling[3], $\beta_2$AR-$G_i$ signaling suppresses changes in calcium handling[51,57], and $\beta_2$AR-$G_i$ signaling is anti-apoptotic[7,8]. While the mechanism that triggers $\beta_2$AR-$G_i$ signaling is unknown, our biochemical observations suggest $Ca^{2+}$ concentrations could directly regulate $\beta_2$AR coupling to $G_i$. It is notable that overexpression of the $Ca^{2+}$/sodium exchanger facilitates $\beta_2$AR-$G_i$ suppression of $\beta_1$AR-$G_s$ signaling[58], and overexpression has been cited to increase the inward LTCC $Ca^{2+}$ current[59].

It is also notable that intracellular $Ca^{2+}$[60,61] and $Mg^{2+}$[61] concentrations rise during ischemia and rise even higher during reperfusion. Whether the rising concentrations affect the G protein subtype specificity of $\beta_2$AR is unknown. However, laboratory-controlled bouts of ischemia and reperfusion have been cited to evoke therapeutic $\beta_2$AR-$G_i$ signaling, i.e. reduce necrosis during a heart attack[9].

Whether negatively charged phospholipids affect $G_i$ interaction with other $G_i$-coupled GPCRs is not known. The observation that $Ca^{2+}$ sensing receptor (CaSR) switches from Gq to $G_i$ after cytosolic $Ca^{2+}$ increases[62] is potentially relevant to our findings.

In conclusion, we show that local membrane charge differentially modulates $\beta_2$AR interaction with competing G protein subtypes ($G_s$ and $G_i$). This discovery expands our knowledge of mechanisms that regulate the G protein coupling selectivity of GPCRs.

## Online Methods

**Heterotrimeric G protein and $\beta_2$AR purification.** All G proteins were heterotrimeric G proteins. $G_s$ heterotrimer (WT $G\alpha_{s\ short}$, his6-3C-$\beta_1$, WT $\gamma_2$) and $G_i$ heterotrimer (WT $G\alpha_{i1-3}$, his6-3C-$\beta_1$, WT $\gamma_2$) and all G protein mutants were expressed and purified as previously described[63]. The $G_{i3}$-$G_s$ chimera was constructed by replacing residues 1-38 of WT $G\alpha_s$ with residues 1-31 of WT $G\alpha_{i3}$. The $G_s$-neg. mutant was constructed by replacing the sequence EDGE (residues 25-28) of WT $G\alpha_s$ with the sequence KDKQ. The $G_{i3}$-pos. mutant was constructed by replacing the sequence KDKQ (residues 32-35) of WT $G\alpha_{i3}$ to the sequence EDGE. The $\beta_2$AR construct was PN1. The construct, expression, purification, and monobromobimane labeling have been described[24]. Labeling efficiency was ~80-100%, as determined by spectroscopic analysis. Purified $\beta_2$AR and G protein were dephosphorylated using Lambda Protein Phosphatase (Lambda PP, New England BioLabs, NEB). Where indicated, $\beta_2$AR was phosphorylated with Protein Kinase A (PKA, NEB) in purification buffer supplemented with 0.1 mM EDTA and 20 μM ATP. (Subsequently, EDTA/ATP were removed by dialysis). Phosphorylation was assessed using the Pro-Q Diamond Phosphoprotein Gel Stain (ThermoFisher Scientific), per the manufacturer's instructions.

**Micelle Composition.** n-dodecyl-β-D-maltopyranoside (DDM), Cholesteryl hemisuccinate (CHS), and 1-palmitoyl-2-oleoyl-(PE,PC,PG,PS) lipids (Avanti Polar Lipids) were mixed in the indicated ratios and solubilized in chloroform. Chloroform was evaporated, and films were re-suspended in 20 mM HEPES (pH 7.4), 100 mM NaCl.

**Fluorescence Spectroscopy.** In experiments examining $\beta_2$AR in micelles, mB-$\beta_2$AR was pre-incubated (30 min room temperature) in micelle stock prior to dilution with other reaction components. Buffer (containing 100 mM NaCl, +/- ligand, +/- CaCl2 or MgCl2), and G protein were sequentially included. Mixtures were incubated 2.5 – 3.0 h at room temperature. Final mB-$\beta_2$AR concentration was 100-500 nM. Emission spectra were read at 22 degrees Celsius using Flurolog-3 or Spex FluoroMax-3 spectrofluorometers (Horiba Jobin Yvon Inc.). (Bandpass = 4 nm; Excitation = 370 nm; Emission = 420-500 nm.) Raw S1c/R1c spectra were smoothed using Prism (GraphPad Software) (n=15 neighbors, 2$^{nd}$ order polynomial). Lambda max is defined as the wavelength at which fluorescence emission is maximum. To determine the $EC_{50}$, curves were fit to the "agonist vs. response" model in Prism 7.0d software.

**GTP Turnover.** Samples were prepared as they were for fluorescence spectroscopy. Following the incubation with G protein, 1 μM GTP/5 μM GDP mixtures were added. Reactions contained: 20 mM HEPES (pH 7.4), 100 mM NaCl, 0.25 μM $G_{i3}$, 0.5 or 1.0 μM $\beta_2$AR (per legend), 200 μM epinephrine, and 4:1 DDM:Lipid. 12 minutes after GTP was added, free GTP was assessed using the GTPase-Glo assay (Promega), which reports free GTP concentration using a luminescence readout. Luminescence was detected using a SpectraMax Paradigm plate reader equipped with a TUNE SpectraMax detection

cartridge (Molecular Devices). Background luminescence was subtracted from experimental reactions.

**Statistics.** Two-sided parametric paired student's *t*-tests were performed using Graphpad Prism7.0d. When comparing lambda max +/- CaCl2, *t*-test calculation assumed all data within a panel were sampled from populations with the same scatter.

**Electrostatic Modeling:** Structural views and mutant models were generated using PyMOL (Schrödinger, LLC). We selected rotomer positions that most closely matched those seen in PDB 3SN6 (for "$G_{i3}$-pos." model) and PDB 1GP2 (for "$G_s$-neg." model). Continuum electrostatics models were calculated using the APBS[64] plugin (MG Lerner, University of Michigan, Ann Arbor) for PyMOL. Atomic charge and radii were calculated using the online PDB2PQR server[65] (pH 7.4, PARSE force field, hydrogen bond optimization, clash avoidance).

**Nanodisc Reagents.** 1,2-dioleoyl-(PE,PC,PG,PS) lipids (Avanti Polar Lipids) were used because of their low phase transition temperature. MSP1E3D1 (Addgene #20066) was expressed and purified as described[66].

**Nanodisc Reconstitution:** Reconstitution was performed as described[24] with the following modifications: Nanodiscs were formed with one lipid type (i.e. 100% DOPS, DOPG, DOPE, or DOPC). The Lipid-to-MSP1E3D1 ratio was 35:1. The MSP1E3D1-to-mB-$\beta_2$AR ratio was 1:10. Empty nanodiscs were separated from nanodiscs containing mB-$\beta_2$AR using M1-anti-FLAG immunoaffinity chromatography in the presence of 2 mM CaCl2, which captures the FLAG-tagged PN1 mB-$\beta_2$AR construct. Eluate was incubated with 5 mM EDTA > 1.5 h at 4 degrees Celsius to remove divalent cations. Subsequently,

samples were injected into a Superdex 200 10/300GL size-exclusion column (GE Healthcare) and the main peak was harvested. The concentration of nanodisc $\beta_2$AR was approximated by SDS-PAGE, using detergent purified $\beta_2$AR of known concentration as a reference.

**Acknowledgements**

We thank Betsy White for assistance with G protein and $\beta_2$AR expression.

This work was supported by National Institutes of Health grants R01NS028471 and R01GM083118 (B.K.K.). B.K.K. is supported by the Chan Zuckerberg Biohub. D.H. was supported by the German Academic Exchange Service (DAAD). M.M. was supported by the American Heart Association Postdoctoral fellowship (17POST33410958).

**Author contributions**

M.J.S designed, performed, and interpreted the research, and wrote the manuscript. B.K.K. championed the investigation, advised on the project, and edited the manuscript. M.J.S performed the purification, labeling, nanodisc reconstitution, and all of the experiments, and S.M., D.H., M.M., and Y.D. provided valuable technical assistance as described: S.M. advised on cloning and provided G protein for pilot experiments. D.H. advised on G protein purification and the GTP turnover assay. M.M. advised on nanodisc reconstitution and provided MSP1E3D1 protein. Y.D. collaborated on pilot experiments not included.

**Competing Interests Statement**

None declared

## REFERENCES


1. Hauser, A.S., Attwood, M.M., Rask-Andersen, M., Schioth, H.B. & Gloriam, D.E. Trends in GPCR drug discovery: new agents, targets and indications. *Nat Rev Drug Discov* **16**, 829-842 (2017).
2. Flock, T. et al. Selectivity determinants of GPCR-G-protein binding. *Nature* **545**, 317-322 (2017).
3. Devic, E., Xiang, Y., Gould, D. & Kobilka, B. beta-adrenergic receptor subtype-specific signaling in cardiac myocytes from beta(1) and beta(2) adrenoceptor knockout mice. *Molecular Pharmacology* **60**, 577-583 (2001).
4. Xiang, Y., Devic, E. & Kobilka, B. The PDZ binding motif of the beta 1 adrenergic receptor modulates receptor trafficking and signaling in cardiac myocytes. *J Biol Chem* **277**, 33783-90 (2002).
5. Xiang, Y. & Kobilka, B. The PDZ-binding motif of the  2-adrenoceptor is essential for physiologic signaling and trafficking in cardiac myocytes. *Proceedings of the National Academy of Sciences* **100**, 10776-10781 (2003).
6. Wang, Y. et al. Norepinephrine- and epinephrine-induced distinct beta2-adrenoceptor signaling is dictated by GRK2 phosphorylation in cardiomyocytes. *J Biol Chem* **283**, 1799-807 (2008).
7. Zhu, W.Z. et al. Dual modulation of cell survival and cell death by beta(2)-adrenergic signaling in adult mouse cardiac myocytes. *Proc Natl Acad Sci U S A* **98**, 1607-12 (2001).
8. Chesley, A. et al. The beta(2)-adrenergic receptor delivers an antiapoptotic signal to cardiac myocytes through G(i)-dependent coupling to phosphatidylinositol 3'-kinase. *Circ Res* **87**, 1172-9 (2000).
9. Tong, H., Bernstein, D., Murphy, E. & Steenbergen, C. The role of beta-adrenergic receptor signaling in cardioprotection. *Faseb j* **19**, 983-5 (2005).
10. Fajardo, G. et al. Deletion of the beta2-adrenergic receptor prevents the development of cardiomyopathy in mice. *J Mol Cell Cardiol* **63**, 155-64 (2013).
11. Paur, H. et al. High levels of circulating epinephrine trigger apical cardiodepression in a beta2-adrenergic receptor/Gi-dependent manner: a new model of Takotsubo cardiomyopathy. *Circulation* **126**, 697-706 (2012).
12. Shao, Y. et al. Novel rat model reveals important roles of beta-adrenoreceptors in stress-induced cardiomyopathy. *Int J Cardiol* **168**, 1943-50 (2013).
13. Vittone, L., Said, M. & Mattiazzi, A. beta 2-Adrenergic stimulation is involved in the contractile dysfunction of the stunned heart. *Naunyn Schmiedebergs Arch Pharmacol* **373**, 60-70 (2006).
14. Bohm, M. et al. Radioimmunochemical quantification of Gi alpha in right and left ventricles from patients with ischaemic and dilated cardiomyopathy and predominant left ventricular failure. *J Mol Cell Cardiol* **26**, 133-49 (1994).
15. Feldman, A.M. et al. Increase of the 40,000-mol wt pertussis toxin substrate (G protein) in the failing human heart. *J Clin Invest* **82**, 189-97 (1988).
16. Eschenhagen, T. et al. Increased messenger RNA level of the inhibitory G protein alpha subunit Gi alpha-2 in human end-stage heart failure. *Circ Res* **70**, 688-96 (1992).
17. Bristow, M.R. et al. Decreased catecholamine sensitivity and beta-adrenergic-receptor density in failing human hearts. *N Engl J Med* **307**, 205-11 (1982).

18. Bristow, M.R. et al. Beta 1- and beta 2-adrenergic-receptor subpopulations in nonfailing and failing human ventricular myocardium: coupling of both receptor subtypes to muscle contraction and selective beta 1-receptor down-regulation in heart failure. *Circ Res* **59**, 297-309 (1986).
19. Bristow, M.R., Hershberger, R.E., Port, J.D., Minobe, W. & Rasmussen, R. Beta 1- and beta 2-adrenergic receptor-mediated adenylate cyclase stimulation in nonfailing and failing human ventricular myocardium. *Mol Pharmacol* **35**, 295-303 (1989).
20. Bristow, M.R. et al. Reduced beta 1 receptor messenger RNA abundance in the failing human heart. *J Clin Invest* **92**, 2737-45 (1993).
21. Zamah, A.M., Delahunty, M., Luttrell, L.M. & Lefkowitz, R.J. Protein Kinase A-mediated Phosphorylation of the beta 2-Adrenergic Receptor Regulates Its Coupling to Gs and Gi. DEMONSTRATION IN A RECONSTITUTED SYSTEM. *Journal of Biological Chemistry* **277**, 31249-31256 (2002).
22. Lefkowitz, R.J., Daaka, Y. & Luttrell, L.M. Switching of the coupling of the beta2-adrenergic receptor to different G proteins by protein kinase A. *Nature* **390**, 88-91 (1997).
23. Zhu, W. et al. Gi-Biased 2AR Signaling Links GRK2 Upregulation to Heart Failure. *Circulation Research* **110**, 265-274 (2011).
24. Dawaliby, R. et al. Allosteric regulation of G protein-coupled receptor activity by phospholipids. *Nat Chem Biol* **12**, 35-9 (2016).
25. Nygaard, R. et al. The dynamic process of beta(2)-adrenergic receptor activation. *Cell* **152**, 532-42 (2013).
26. Manglik, A. et al. Structural Insights into the Dynamic Process of beta2-Adrenergic Receptor Signaling. *Cell* **161**, 1101-1111 (2015).
27. Rasmussen, S.G. et al. Crystal structure of the beta2 adrenergic receptor-Gs protein complex. *Nature* **477**, 549-55 (2011).
28. Yao, X.J. et al. The effect of ligand efficacy on the formation and stability of a GPCR-G protein complex. *Proc Natl Acad Sci U S A* **106**, 9501-6 (2009).
29. Hafez, I.M. & Cullis, P.R. Cholesteryl hemisuccinate exhibits pH sensitive polymorphic phase behavior. *Biochim Biophys Acta* **1463**, 107-14 (2000).
30. Shi, X. et al. Ca2+ regulates T-cell receptor activation by modulating the charge property of lipids. *Nature* **493**, 111-5 (2013).
31. Crouthamel, M., Thiyagarajan, M.M., Evanko, D.S. & Wedegaertner, P.B. N-terminal polybasic motifs are required for plasma membrane localization of Galpha(s) and Galpha(q). *Cell Signal* **20**, 1900-10 (2008).
32. Her, C. et al. The Charge Properties of Phospholipid Nanodiscs. *Biophys J* **111**, 989-98 (2016).
33. Rybin, V.O., Xu, X., Lisanti, M.P. & Steinberg, S.F. Differential targeting of beta -adrenergic receptor subtypes and adenylyl cyclase to cardiomyocyte caveolae. A mechanism to functionally regulate the cAMP signaling pathway. *J Biol Chem* **275**, 41447-57 (2000).
34. Xiang, Y. Caveolar Localization Dictates Physiologic Signaling of beta 2-Adrenoceptors in Neonatal Cardiac Myocytes. *Journal of Biological Chemistry* **277**, 34280-34286 (2002).
35. Nikolaev, V.O. et al. Beta2-adrenergic receptor redistribution in heart failure changes cAMP compartmentation. *Science* **327**, 1653-7 (2010).
36. Rosemblatt, M., Hidalgo, C., Vergara, C. & Ikemoto, N. Immunological and biochemical properties of transverse tubule membranes isolated from rabbit skeletal muscle. *J Biol Chem* **256**, 8140-8 (1981).

37. Lau, Y.H., Caswell, A.H., Brunschwig, J.P., Baerwald, R. & Garcia, M. Lipid analysis and freeze-fracture studies on isolated transverse tubules and sarcoplasmic reticulum subfractions of skeletal muscle. *J Biol Chem* **254**, 540-6 (1979).
38. Pediconi, M.F., Donoso, P., Hidalgo, C. & Barrantes, F.J. Lipid composition of purified transverse tubule membranes isolated from amphibian skeletal muscle. *Biochim Biophys Acta* **921**, 398-404 (1987).
39. Post, J.A., Langer, G.A., Op den Kamp, J.A. & Verkleij, A.J. Phospholipid asymmetry in cardiac sarcolemma. Analysis of intact cells and 'gas-dissected' membranes. *Biochim Biophys Acta* **943**, 256-66 (1988).
40. Post, J.A., Verkleij, A.J. & Langer, G.A. Organization and function of sarcolemmal phospholipids in control and ischemic/reperfused cardiomyocytes. *J Mol Cell Cardiol* **27**, 749-60 (1995).
41. Fearnley, C.J., Roderick, H.L. & Bootman, M.D. Calcium signaling in cardiac myocytes. *Cold Spring Harb Perspect Biol* **3**, a004242 (2011).
42. Louch, W.E., Stokke, M.K., Sjaastad, I., Christensen, G. & Sejersted, O.M. No rest for the weary: diastolic calcium homeostasis in the normal and failing myocardium. *Physiology (Bethesda)* **27**, 308-23 (2012).
43. Verkleij, A.J. & Post, J.A. Membrane phospholipid asymmetry and signal transduction. *J Membr Biol* **178**, 1-10 (2000).
44. Houser, S.R. & Molkentin, J.D. Does contractile Ca2+ control calcineurin-NFAT signaling and pathological hypertrophy in cardiac myocytes? *Sci Signal* **1**, pe31 (2008).
45. Langer, G.A. & Peskoff, A. Calcium concentration and movement in the diadic cleft space of the cardiac ventricular cell. *Biophys J* **70**, 1169-82 (1996).
46. Peskoff, A. & Langer, G.A. Calcium concentration and movement in the ventricular cardiac cell during an excitation-contraction cycle. *Biophys J* **74**, 153-74 (1998).
47. Philipson, K.D., Bers, D.M. & Nishimoto, A.Y. The role of phospholipids in the Ca2+ binding of isolated cardiac sarcolemma. *J Mol Cell Cardiol* **12**, 1159-73 (1980).
48. Boettcher, J.M. et al. Atomic view of calcium-induced clustering of phosphatidylserine in mixed lipid bilayers. *Biochemistry* **50**, 2264-73 (2011).
49. Haverstick, D.M. & Glaser, M. Visualization of Ca2+-induced phospholipid domains. *Proc Natl Acad Sci U S A* **84**, 4475-9 (1987).
50. Wang, Y.H., Slochower, D.R. & Janmey, P.A. Counterion-mediated cluster formation by polyphosphoinositides. *Chem Phys Lipids* **182**, 38-51 (2014).
51. Zhu, W., Zeng, X., Zheng, M. & Xiao, R.P. The enigma of beta2-adrenergic receptor Gi signaling in the heart: the good, the bad, and the ugly. *Circ Res* **97**, 507-9 (2005).
52. Schmid, E. et al. Cardiac RKIP induces a beneficial beta-adrenoceptor-dependent positive inotropy. *Nat Med* **21**, 1298-306 (2015).
53. Woo, A.Y., Song, Y., Xiao, R.P. & Zhu, W. Biased beta2-adrenoceptor signalling in heart failure: pathophysiology and drug discovery. *Br J Pharmacol* **172**, 5444-56 (2015).
54. Bayeva, M., Sawicki, K.T., Butler, J., Gheorghiade, M. & Ardehali, H. Molecular and cellular basis of viable dysfunctional myocardium. *Circ Heart Fail* **7**, 680-91 (2014).
55. Waagstein, F. & Rutherford, J.D. The Evolution of the Use of beta-Blockers to Treat Heart Failure: A Conversation With Finn Waagstein, MD. *Circulation* **136**, 889-893 (2017).

56. Kehat, I. & Molkentin, J.D. Molecular pathways underlying cardiac remodeling during pathophysiological stimulation. *Circulation* **122**, 2727-35 (2010).
57. Xiao, R.P., Ji, X.W. & Lakatta, E.G. Functional Coupling of the Beta(2)-Adrenoceptor to a Pertussis-Toxin-Sensitive G-Protein in Cardiac Myocytes. *Molecular Pharmacology* **47**, 322-329 (1995).
58. Sato, M., Gong, H., Terracciano, C.M., Ranu, H. & Harding, S.E. Loss of beta-adrenoceptor response in myocytes overexpressing the Na+/Ca(2+)-exchanger. *J Mol Cell Cardiol* **36**, 43-8 (2004).
59. Ottolia, M., Torres, N., Bridge, J.H., Philipson, K.D. & Goldhaber, J.I. Na/Ca exchange and contraction of the heart. *J Mol Cell Cardiol* **61**, 28-33 (2013).
60. Kalogeris, T., Baines, C.P., Krenz, M. & Korthuis, R.J. Cell biology of ischemia/reperfusion injury. *Int Rev Cell Mol Biol* **298**, 229-317 (2012).
61. Murphy, E. & Steenbergen, C. Ion transport and energetics during cell death and protection. *Physiology (Bethesda)* **23**, 115-23 (2008).
62. Conigrave, A.D. The Calcium-Sensing Receptor and the Parathyroid: Past, Present, Future. *Front Physiol* **7**, 563 (2016).
63. Gregorio, G.G. et al. Single-molecule analysis of ligand efficacy in beta2AR-G-protein activation. *Nature* **547**, 68-73 (2017).
64. Baker, N.A., Sept, D., Joseph, S., Holst, M.J. & McCammon, J.A. Electrostatics of nanosystems: application to microtubules and the ribosome. *Proc Natl Acad Sci U S A* **98**, 10037-41 (2001).
65. Dolinsky, T.J., Nielsen, J.E., McCammon, J.A. & Baker, N.A. PDB2PQR: an automated pipeline for the setup of Poisson-Boltzmann electrostatics calculations. *Nucleic Acids Res* **32**, W665-7 (2004).
66. Velez-Ruiz, G.A. & Sunahara, R.K. Reconstitution of G protein-coupled receptors into a model bilayer system: reconstituted high-density lipoprotein particles. *Methods Mol Biol* **756**, 167-82 (2011).